

BELLCOMM, INC.

1100 Seventeenth Street, N.W. Washington, D. C. 20036

SUBJECT: A New Concept in Heat Shield
Design - Deployable Heat
Shield - Case 710

DATE: May 10, 1968

FROM: C. P. Wang

ABSTRACT

A new concept in heat shield design is described in which the main spacecraft is effectively "hidden" in the wake of a torus-shaped heat shield. This heat shield increases the shock stand-off distance and enhances the "radiation-cooling effect," such that the kinetic energy of the combined entry vehicle is sufficiently attenuated without heating up the main spacecraft. The flow patterns of both a hypersonic sphere and hypersonic torus are described to illustrate the effect.

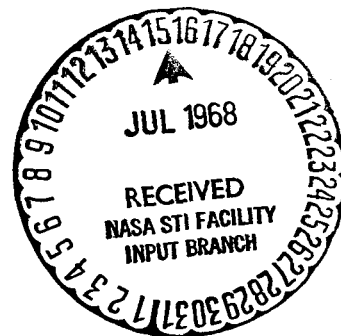
(NASA-CR-95528) A NEW CONCEPT IN HEAT
SHIELD DESIGN DEPLOYABLE HEAT SHIELD
(Bellcomm, Inc.) 20 p

N79-72326

Unclas
11224

00/18

| | | |
|------------|---|------------|
| FF No. 60: | <i>CR-95528</i> | |
| | (NASA CR OR TMX OR AD NUMBER) | (CATEGORY) |
| | AVAILABLE TO NASA OFFICIALS NASA | |



BELLCOMM, INC.

1100 Seventeenth Street, N.W. Washington, D. C. 20036

SUBJECT: A New Concept in Heat Shield
Design - Deployable Heat
Shield - Case 710

DATE: May 10, 1968

FROM: C. P. Wang

MEMORANDUM FOR FILE

INTRODUCTION

Atmosphere entry speeds of planetary probes, such as might be used in the exploration of Mars or Venus, can be significantly above parabolic speed. In minimum-energy (Hohmann) transfer, the entry speeds are only slightly in excess of parabolic (38 k-ft/sec), but these trajectories require long trip times (typically 259 days for Mars and 146 days for Venus). Entry speeds will be significantly above parabolic if the trip times are shortened. A principal consideration at such high speeds is the heating problem. The problem is whether the entry vehicle can survive heating at such speeds and if so, how severe a penalty is paid in terms of weight of the vehicle heat shield.

To illustrate the severity of the heating problem associated with higher entry speeds, consider a simple spherical entry vehicle of one foot radius and ballistic coefficient 50 lb/ft^2 in vertical entry into the earth's atmosphere. The total heating load on the entry vehicle is plotted against the entry speed in Figure 1.* Due to the emissivity of the gas which varies as the gas temperature, density, and composition, the radiative contribution to the heating may vary with velocity by as much as the 15th power. Hence, although for entry from low altitude earth orbit the radiative contribution in the case of a blunt body is usually negligible, it tends to become overwhelming at speeds in excess of earth parabolic speed.

The basic mechanisms involved in the heating process are mainly convective heating (or frictional heating) and radiative heating. At relatively low speeds, the frictional force exerted on a vehicle surface is directly related to the process by which heat can be convected to that surface. The

*Actually the total heating load is lower than the approximation represented in this curve, due to effects of self-absorption and radiation-cooling.

incremental quantity of energy in the form of heat, δH , convected to an entry vehicle, is related to the incremental change in kinetic energy of the entry vehicle δE by

$$\delta H \sim \frac{F}{D} \delta E$$

where F is the total frictional force exerted on the vehicle surface, and D is the total drag force experienced by the vehicle. To minimize the convective heating, a vehicle is shaped such that the ratio of frictional force to total drag force is the minimal. Thus the blunt shapes, for which the pressure drag is high, are commonly chosen for entry vehicles.

Since the gas enthalpy behind the bow shock is proportional to the square of the vehicle flight Mach number, or the square of the entry speed, the shock layer (i.e. the layer between the bow shock and the entry vehicle) at higher entry speeds becomes hot and highly excited. The air which enters this shock layer undergoes such high molecular excitations that it becomes an intense source of radiation. Because this radiation source is so close to the vehicle surface, approximately half of the radiative energy is absorbed by the vehicle while less than a few percent of the total heat (gas enthalpy) is absorbed by the vehicle through convection.

Up to the present time entry speeds from earth orbit have been sufficiently low that heating has been essentially a convective process. Blunt shaped entry bodies, employing ablative heat shields, have been successfully protected from convective heating. At the higher entry speeds desired in the future, it appears difficult to prevent the rapid increase in radiative heating of a blunt body by means of an ablative heat shield alone. Therefore, it is important to re-examine the effect of vehicle shape or heat shield configuration when radiative contributions to heating are dominant. Allen¹ et al., suggested the use of conical shaped bodies to reduce radiative heating, but this incurs the penalty of increasing the convective heating, which has to be fended off by ablation or mass injection. This results in high mass loss or high heat shield weight.

A new concept in heat shield configuration consisting of a torus-shaped deployable heat shield in front of the main vehicle, shown in Figure 2, is proposed. Because of the small solid angle subtended by the radiative heat source with respect to the main vehicle, and because of the large "radiation-cooling effect," both the radiative and convective heat transfer to the main vehicle are reduced in this configuration. To illustrate these effects further, the flow fields around a sphere and around a torus-shaped body have been investigated.

Flow Field Around a Hypersonic Sphere

The flow field of a hypersonic reentry blunt body in the continuum regime has been studied extensively in the last decade. A qualitative description of the flow pattern is shown in Figure 3. The intense compressional heating and deceleration of the gas are accomplished by the detached bow shock in front of the body. Upon traversing this shock, the gas enters the shock layer which is, in fact, the high-temperature environmental source for the heat transfer to the body. The temperature, density, and volume of this heat source are important in determining the heat transfer to the body. The temperature and the density are dependent on the entry velocity and the composition and density of the atmosphere. For a frozen flow in air, this temperature and density are obtained from the Rankine-Hugoniot relations, as follows;

$$\frac{\rho_2}{\rho_1} = \frac{M_1^2}{1 + \frac{\gamma-1}{\gamma+1}(M_1^2-1)} \approx 6, \text{ for } M_1 \gg 1 \quad (1)$$

$$\frac{T_2}{T_1} = 1 + \frac{2(\gamma-1)}{(\gamma+1)^2} \frac{(M_1^2-1)(1+\gamma M_1^2)}{M_1^2} \approx \frac{7}{36} M_1^2 \quad (2)$$

where ρ_1 and T_1 are free-stream density and temperature in front of the bow shock, ρ_2 and T_2 are density and temperature in the shock layer behind the bow shock, γ is the ratio of specific heats, and M_1 is the vehicle flight Mach number. The volume of this heat source is proportional to the stand-off distance Δ (the distance between the bow shock and the body). This distance is a function of the radius of curvature, R , of the nose and the gas density ratio across the shock wave, ρ_1/ρ_2 . Approximately,

$$\Delta \sim R \frac{\rho_1}{\rho_2} \quad (3)$$

To a good approximation the convective heat flux at the stagnation point, \dot{q}_c , depends on the gas density ρ_1 , body velocity u , and body radius R , as*

$$\dot{q}_c \sim \left(\frac{\rho_1}{R} \right)^{1/2} u^3 \quad (4)$$

Radiative heat transfer at the stagnation point is estimated to vary as¹

$$\dot{q}_r \sim \rho_1^{3/2} R u^n \quad (5)$$

where n ranges from 5 up to 15 and depends on the composition of the gas. From the Equations (4) and (5), it is evident that, at high body velocity, the radiative heat transfer becomes overwhelmingly important.

Around the body, the gas is first compressed by the shock wave, and then expands to a low pressure (still greater than ambient) by Prandtl-Meyer expansion waves. At the base of the body there is shear flow between the viscous circulating (or base flow) region and the inviscid outer wake, this shear layer being made up predominantly of boundary layer fluid. The shear layer converges on the center line, eventually undergoing normal shock at the "neck" of this flow, from which an oblique "wake shock" develops, ultimately forming a viscous core or inner wake. Fluid in the inviscid wake crosses the wake shock, increasing its pressure, temperature and density. In continuing downstream this outer wake merges with the inner wake.

*A laminar boundary layer is assumed. For other assumptions and derivations see Reference 2.

Moreover, the electrons generated by the bow shock in front of the blunt body, and by the deceleration and heating of the gas at the neck, shield the body from electromagnetic radiation, causing communications blackout.

The distribution of parameters in this flow field is the result of a complex interaction of body velocity, body shape, chemical kinetics and boundary layer transition. Exact solutions are extremely difficult, if not impossible to obtain. There are several methods of approximation, such as are given in References 3 and 4.

Flow Around a Hypersonic Torus Moving Along Its Axis of Symmetry

In the flow field of a hypersonic torus, similar to the hypersonic sphere case discussed above, there is a detached bow shock in front of the torus body, a shock layer, expansion waves, free shear layer, base flow, neck, wake shock, outer wake, inner wake, etc., as is shown in Figure 4.* However, the bow shock in the center part of the torus is sucked in and forms an important and complicated "shock interaction" region, where Mach reflections, slipstreams, interactions of shock waves and expansion waves, etc., occur. Presumably, the shock interaction region is a high temperature, high density, non-uniform non-equilibrium region.

Initially, as the gas molecules enter the region, they will reach a high translational temperature and a high degree of electronic excitation, resulting in intense radiative emission. As the molecules undergo collision, the remaining inner degrees of freedom will be excited, and dissociation and ionization will follow. The gas will finally reach its state of thermochemical equilibrium, and the emission will decay to its equilibrium level.

The flow behind the shock interaction region, the "center wake," is subsonic and relatively cold. Hence both convective and radiative heat fluxes to a body "hidden" in the center wake are significantly reduced. Due to the complexity of the problem, only order of magnitude estimates will be given to demonstrate these effects.

Assuming the shock interaction region is one of isoenergetic, grey and transparent gas then, as is shown by

*This qualitative flow pattern is obtained by assuming a two-dimensional flow, and using the oblique-shock relations, the Prandtl-Meyer expansion, the shock polar, and the pressure matching technique.

Kourganoff⁵, the total energy emission rate per unit volume of gas at a temperature T and density ρ is

$$\dot{E}_r = 4\pi\rho \int_0^{\infty} K_\nu B_\nu d\nu \quad (6)$$

where: $B_\nu = \frac{4\pi h^3 \nu^3}{c^2} \frac{1}{e^{h\nu/kT} - 1}$ Planck Law

K_ν = mass absorption coefficient

$2\pi h$ = Planck constant

k = Boltzmann constant

c = speed of light

ν = radiation frequency

Defining the Planck mean mass absorption coefficient K by

$$K = \frac{4\pi \int_0^{\infty} B_\nu K_\nu d\nu}{4\pi \int_0^{\infty} B_\nu d\nu} = \frac{\dot{E}_r/\rho}{4\sigma T^4}$$

where

$$\sigma = \frac{\pi^2 k^4}{60c^2 h^3}, \text{ Stefan-Boltzmann constant}$$

The emission rate is given by

$$\dot{E}_r = 4\rho\sigma KT^4. \quad (7)$$

Note that K is a strong function of gas temperature and composition. For example,

$$\frac{1}{2} \rho K = 0.138 \left(\frac{\rho}{\rho_0} \right)^{1.28} \left(\frac{T}{10^4} \right)^{6.54} \text{ cm}^{-1}$$

where ρ_0 is the air density at sea level, and T is the gas temperature in $^{\circ}\text{K}$. The above equation is a good approximation for air between 8000°K and $16,000^{\circ}\text{K}$.⁶

As mentioned before, the flow field in the shock interaction region is very complex, even without radiation. However, in order to estimate the radiation-cooling effect and the radiative heat transfer, an exceedingly simplified model is used to estimate the temperature profile in the shock interaction region. In this model, the following assumptions are made: the shock interaction region is an optically thin plane layer of incompressible gas extending to infinity in the direction normal to the flow, and the gas entering the shock interaction region is heated to the frozen temperature by adiabatic shock heating (Equation 2) and relaxes to a lower temperature by radiation only. Under these assumptions, the equation of energy conservation is simply the balance between radiation loss E_r (Equation 7) and the change of enthalpy of the gas $\rho \frac{dh}{dt}$, i.e.

$$\rho \frac{dh}{dt} + 4\rho K \sigma T^4 = 0 \quad (8)$$

following the gas molecules, $dt = \frac{dx}{u_2}$, where $x = 0$ at the center shock and increases toward the vehicle surface, and u_2 is the flow velocity* in the shock interaction region. Using the dimensionless variables

$$\xi = \frac{x}{R} \quad (9)$$

$$\tau = \frac{T}{T_1} \quad (10)$$

*This flow velocity is obtained from the mass continuity equation.

Equation 8 becomes*

$$d\xi + C \frac{d\tau}{\tau^{10.54}} = 0 \quad (11)$$

where

$$C = 3 \times 10^{-3} \left(\frac{\rho_0}{\rho_1} \right)^{1.28} \frac{\rho_1 u_1 C_p T_1}{\left(\frac{T_1}{10^4} \right)^{6.54} \sigma T_1^4 R} \quad (12)$$

C_p = specific heat at constant pressure

R = vehicle radius in ft

ρ_0 = gas density at sea level

ρ_1 , u_1 and T_1 are free-stream gas density, velocity and temperature, respectively.

Integrating Equation 11 from $\xi = 0$; $\tau = \frac{T_2}{T_1}$ to ξ ; τ gives

$$\tau = \frac{T_2}{T_1} \left\{ 1 + \frac{9.54}{C} \left(\frac{T_2}{T_1} \right)^{9.54} \xi \right\}^{-\frac{1}{9.54}} \quad (13)$$

For a typical case, we select a main vehicle radius $R = 1$ ft, with a distance of $3R$ from the torus, and earth entry speed $u_1 = 40,000$ ft/sec at an altitude of 100 k-ft. The resultant temperature near the vehicle surface is about 10% of the temperature just behind the shock wave. Moreover, near the main vehicle surface, $\xi_{b.s.}$,

$$\lim_{u_1 \rightarrow \infty} \tau = \text{constant} \quad (14)$$

*In this calculation the Planck mean absorption coefficient K is obtained from Reference 6.

That is, as the entry speed further increases, the temperature just behind the shock wave increases as the square of the entry speed, but the temperature near the vehicle surface approaches a constant. Therefore, convective heat will only increase as $u^{1/2*}$, instead of as u^3 (Equation 4).

To illustrate the reduction of radiative heating, a comparison of radiative heat flux to the main vehicle with and without the torus in front has been made. The rate at which energy from the radiative heat source of volume dV is absorbed by the surface area dA of a black body, hidden in the center wake, is

$$\dot{q}_r dA = \int_{\text{volume of radiative heat source}} \dot{E}_r \frac{\cos\theta dA}{4\pi d^2} dV \quad (15)$$

where θ is the angle between the ray direction and the surface normal and d is the distance between the radiative source (the shock interaction region) and the surface element. Let θ and x be the two independent coordinate variables, then the volume element is

$$dV = 2\pi x^2 \frac{\sin\theta}{\cos^2\theta} d\theta dx$$

and

$$d = \frac{x}{\cos\theta}$$

$$* \text{Because } \dot{q}_c = \frac{Nu_r k_r (T_w - T_r)}{R}$$

$$\sim \left(\frac{\rho}{R} \frac{u}{\mu}\right)^{1/2} Pr^{5/2} (T_w - T_r) \sim u^{1/2} \text{ for constant } T_r,$$

where Nu_r is the Nusselt number of the flow, k_r is the thermal conductivity of the gas, μ is the viscosity of the gas, Pr is the Prandtl number, and T_w and T_r are surface temperature and recovery temperature, respectively.

Therefore,
$$\int_{\text{Volume}} \dot{E}_r \frac{\cos\theta}{4\pi d^2} dV dA = \iint \dot{E}_r \frac{\sin\theta}{2} d\theta dx dA$$

$$= R \int_{\xi=0}^{\xi=\xi_{b.s.}} \int_{\theta=0}^{\theta=\theta(\xi)} \dot{E}_r \frac{\sin\theta}{2} d\theta d\xi dA$$

where $\xi_{b.s.}$ is the value of ξ at the body surface, and $\theta(\xi)$ is specified by the boundary of the radiation source. Let ϵ be the thickness of the dominant radiative heat source, then

$$R \int_{\xi=0}^{\xi=\xi_{b.s.}} \int_{\theta=0}^{\theta=\theta(\xi)} \dot{E}_r \frac{\sin\theta}{2} d\theta d\xi dA = R \int_{\xi=0}^{\xi=\epsilon} \dot{E}_r d\xi \int_{\theta=0}^{\theta=\theta(0)} \frac{\sin\theta}{2} d\theta dA$$

$$+ R \int_{\xi=\epsilon}^{\xi=\xi_{b.s.}} \int_{\theta=0}^{\theta=\theta(\xi)} \dot{E}_r \frac{\sin\theta}{2} d\theta d\xi dA$$

$$+ O(\epsilon) \quad (16)$$

In the present case, the temperature profile (Equation 13) is such that the dominant contribution of the radiative heat flux comes from a thin layer of thickness ϵ much smaller than 10^{-1} . It can be shown that

$$\int_{\xi=\epsilon}^{\xi=\xi_{b.s.}} \int_{\theta=0}^{\theta=\theta(\xi)} \dot{E}_r \frac{\sin\theta}{2} d\theta d\xi \ll \int_{\xi=0}^{\xi=\epsilon} \dot{E}_r d\xi \int_{\theta=0}^{\theta=\theta(0)} \frac{\sin\theta}{2} d\theta$$

Therefore, it is a good approximation to neglect the second integral on the right-hand side of Equation (16). The radiative heat flux \dot{q}_r to the body surface of unit area is then

$$\dot{q}_r = R \int_{\xi=0}^{\xi=e} \dot{E}_r d\xi \int_{\theta=0}^{\theta=\theta(0)} \frac{\sin\theta}{2} d\theta \quad (17)$$

The integral $\int_0^e \dot{E}_r d\xi$ gives the same value both with the torus and without it if $\frac{T_2}{T_1}$ and the free-stream conditions are the same. It might be argued that the torus will change the ballistic coefficient of the combined entry vehicle, hence $\frac{T_2}{T_1}$ or the free-stream conditions will differ. Since the ballistic coefficient, B , is equal to $\frac{M}{C_D A}$, adding the torus certainly increases the front area, A , and the drag coefficient, C_D . The mass, M , of the combined entry vehicle is also increased. In general, if the averaged specific weight of the torus heat shield is the same as the averaged specific weight of the main vehicle, the ballistic coefficient of the combined vehicle will be 25% lower than the ballistic coefficient of the main vehicle alone. For the case considered here, if a hollow steel torus of 3/16" wall thickness is used, the ballistic coefficient of the combined vehicle will be about 1.4 slug/ft², which is 10% lower than the ballistic coefficient of the main vehicle alone. Since only a small percentage change of the ballistic coefficient occurs, a rough estimation of the effect of $\frac{\Delta B}{B}$ on the maximum radiative heating can easily be obtained. By Equation 7,

$$\dot{E}_r \sim \rho K T^4 \sim \rho^m T^n$$

where m and n are determined by the Planck mean absorption coefficient K . In the present case, $m = 1.28$ and $n = 10.54$. According to Allen and Eggers,⁷

$$V = V_{\epsilon} \exp\left[-\frac{\rho_0}{2\beta B} e^{-\beta y}\right]$$

$$\rho = \rho_0 e^{-\beta y}$$

$$T \sim V^2$$

where V_{ϵ} is the entry velocity, ρ_0 is the sea level density, β is the atmosphere scale height, and y is the altitude. To find the maximum radiative heating, $(\dot{E}_r)_{\max}$, with respect to the altitude, $\frac{\partial \dot{E}_r}{\partial y} = 0$ gives the altitude, y_{\max} , at which $(\dot{E}_r)_{\max}$ occurs. The results are

$$y_{\max} = \frac{1}{\beta} \ln \frac{n\rho_0}{mB\beta}$$

and

$$(\dot{E}_r)_{\max} \sim \frac{m}{n} e^{-m} B$$

Therefore,

$$\frac{\Delta(\dot{E}_r)_{\max}}{(\dot{E}_r)_{\max}} = \frac{\Delta B}{B} \quad (18)$$

That is, a decrease in B will always decrease the radiative heating. By Equation 17, neglecting the changes in ballistic coefficient, the ratio of radiative heat fluxes to the vehicle is simply,

$$\frac{\dot{q}_{r \text{ with torus}}}{\dot{q}_{r \text{ without torus}}} = \frac{\frac{1}{2} \int_0^{\theta(0)} \sin \theta d\theta}{\frac{1}{2} \int_0^{\frac{\pi}{2}} \sin \theta d\theta} = \int_0^{\theta(0)} \sin \theta d\theta$$

For the geometry in Figure 4, where $D/r = 6$, $D = 2R$, and $L = 4R$,
 $\theta(0) = \cos^{-1} \frac{3}{\sqrt{10}}$. Hence

$$\int_0^{\theta(0)} \sin \theta d\theta = .05$$

That is, the radiative heat flux to the main vehicle is reduced by a factor of 20 by hiding it behind the torus heat shield.

Deployable Heat Shield

In view of the above discussion, it is suggested that hiding the main spacecraft in the "cold" center wake of a deployable shielding vehicle may be one way to significantly reduce the radiative heat transfer to the main vehicle.

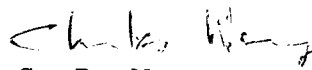
In practice, the torus in front of the entry vehicle can be considered as a deployable heat shield, which is closely attached in front of the main spacecraft before entry, and extended forward and held in position by a few steel trusses during entry as is shown in Figure 2. Furthermore, this deployable heat shield and associated trusses might also be used as a "couch stroke" (or shock absorber) to absorb the kinetic energy of impact for a crushable lander. Other problems under consideration are the strength of materials under high temperature and the stability of the combined vehicle. Since only a fraction of the total drag force is acting on the torus, this alleviates the strength of the material problem. As for the stability problem, it is hoped that the combined vehicle can be stabilized by properly locating the center of gravity and distributing the drag force, without excessive dependence on spin or other means of stabilization.

It is obvious that a body inserted in the center wake will perturb the flow field locally; however, the general flow pattern should not be altered significantly from that shown in Figure 4. Hence the order of magnitude estimates given above should hold. For more accurate calculations concerning this deployable heat shield, many complicated problems have to be solved first. For example, the flow and radiation field in the shock interaction region; the size (or diameter) of the center wake; the temperature, density, and velocity profiles in the center wake; the influence of the perturbing body on the center wake; and how all these depend on the Mach number, gas composition, ambient conditions, torus cross-section radius r , torus diameter D , body size R , and distance between torus and body L , etc. All these need further study and experimental verification.

CONCLUSIONS

It appears that it is possible to generate an extended high temperature and radiative region, sufficiently far from the main vehicle, such that much of the kinetic energy of the combined entry vehicle is radiated away without heating the main spacecraft. The use of a torus in front of an entry vehicle suggests the possibility of solving the radiative and convective heating problem of a high speed entry vehicle.

1014-CPW-jan


C. P. Wang

Attachments
Figures 1-4

BELLCOMM, INC.

REFERENCES

1. Allen, H. J., and Seiff, A., "Aerodynamic Heating of Conical Entry Vehicles at Speeds in Excess of Earth Parabolic Speed," NASA TR-R-185, 1963.
2. Detra, R. W., and Hidalgo, H., "Generalized Heat Transfer Formulas and Graphs for Nose Cone Reentry into Atmosphere," J. American Rocket Society 31, 318 (1961).
3. Bohachevsky, Ihor O., and Mates, Robert E., "A Direct Method for Calculation of Flow About an Axisymmetric Blunt Body at Angle of Attack," AIAA J., 4, 776 (1966).
4. Moretti, G. and Bleich, G., "Three-Dimensional Flow Around Blunt Bodies," presented at AIAA 5th Aerospace Science Meeting, January 1967, New York, N.Y.
5. Kourganoff, V., "Basic Methods in Transfer Problems," Dover Publications, Inc., New York, N.Y., 1963.
6. Thomas, P. D., "Air Emissivity and Shock Layer Radiation," J. Aerospace Science, 29, 477 (1962).
7. Allen, H. J. and Eggers, A. J., Jr., "A Study of the Motion and Aerodynamic Heating of Ballistic Missiles Entering the Earth's Atmosphere at High Supersonic Speeds," NACA Rep. 1381, 1958.

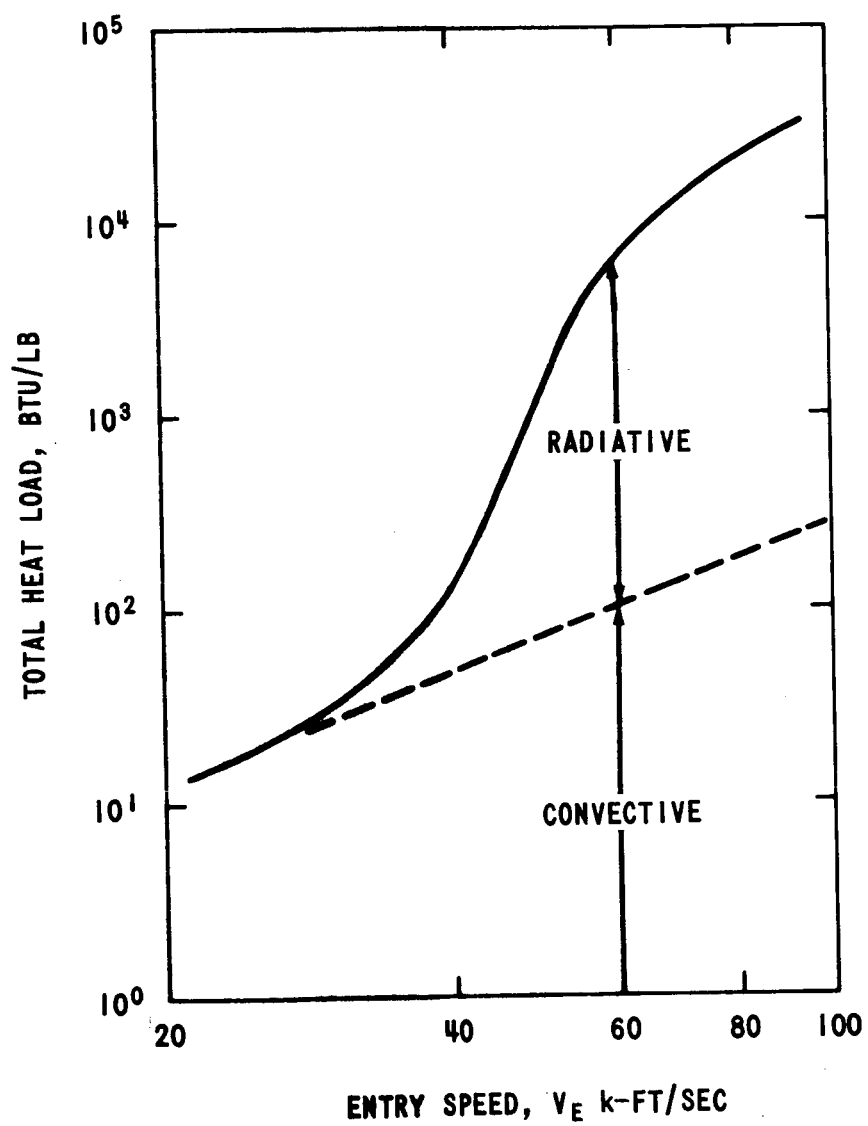
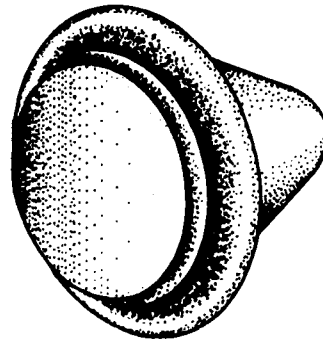
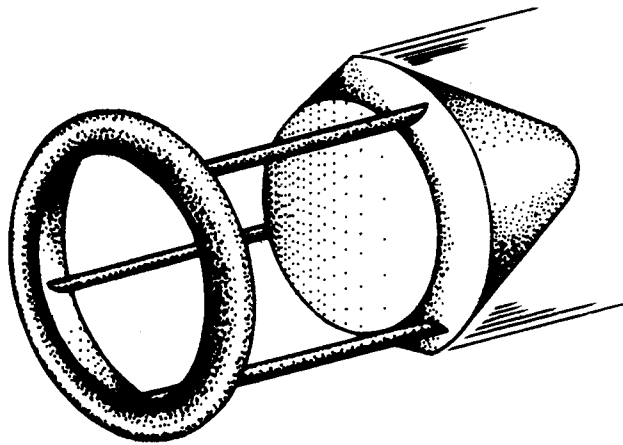


FIGURE 1 - TOTAL HEAT LOAD VERSUS ENTRY SPEED



BEFORE ENTRY



DURING ENTRY

FIGURE 2 - SKETCH OF DEPLOYABLE HEAT SHIELD

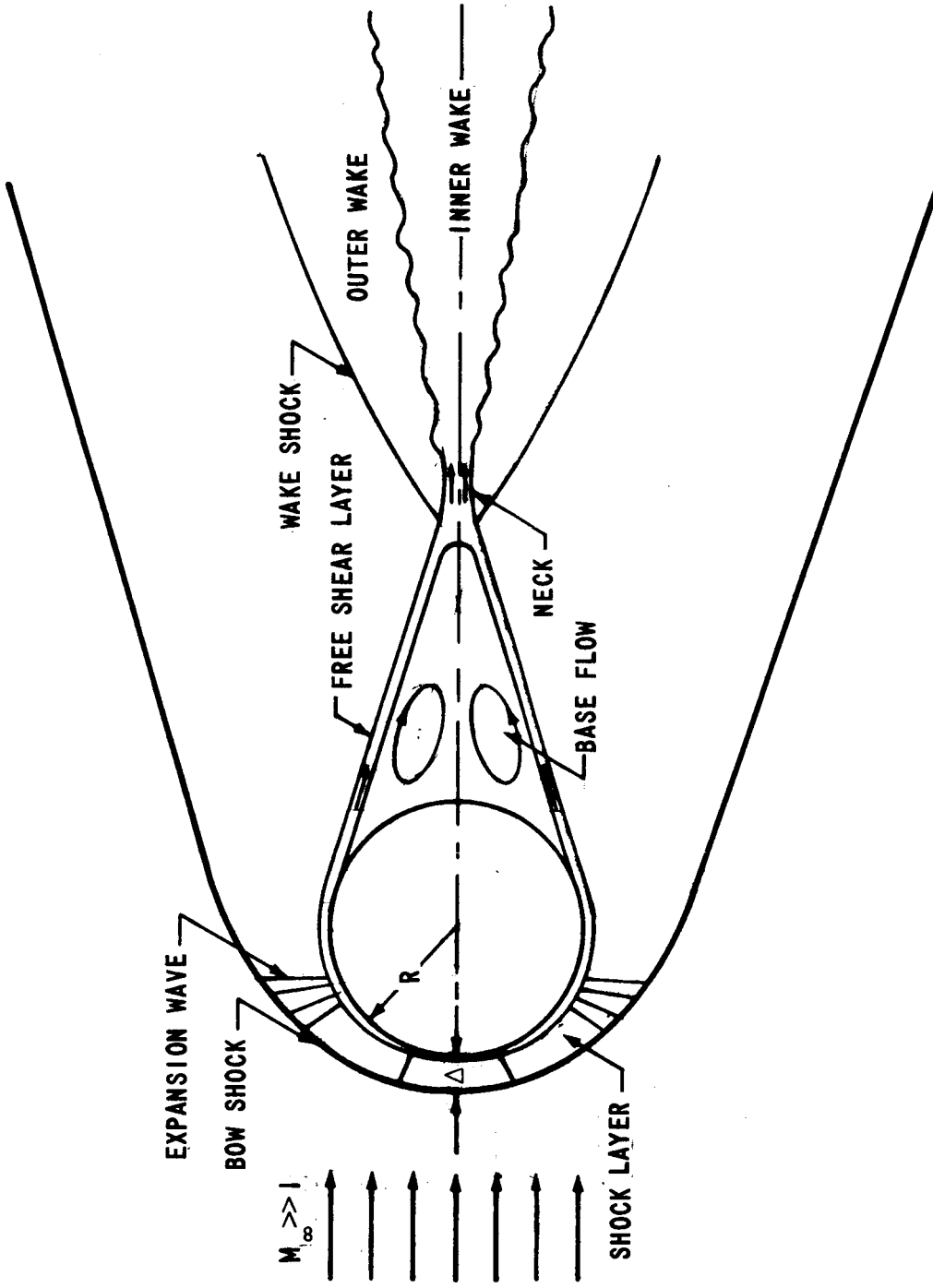


FIGURE 3 - FLOW AROUND A HYPERSONIC SPHERE

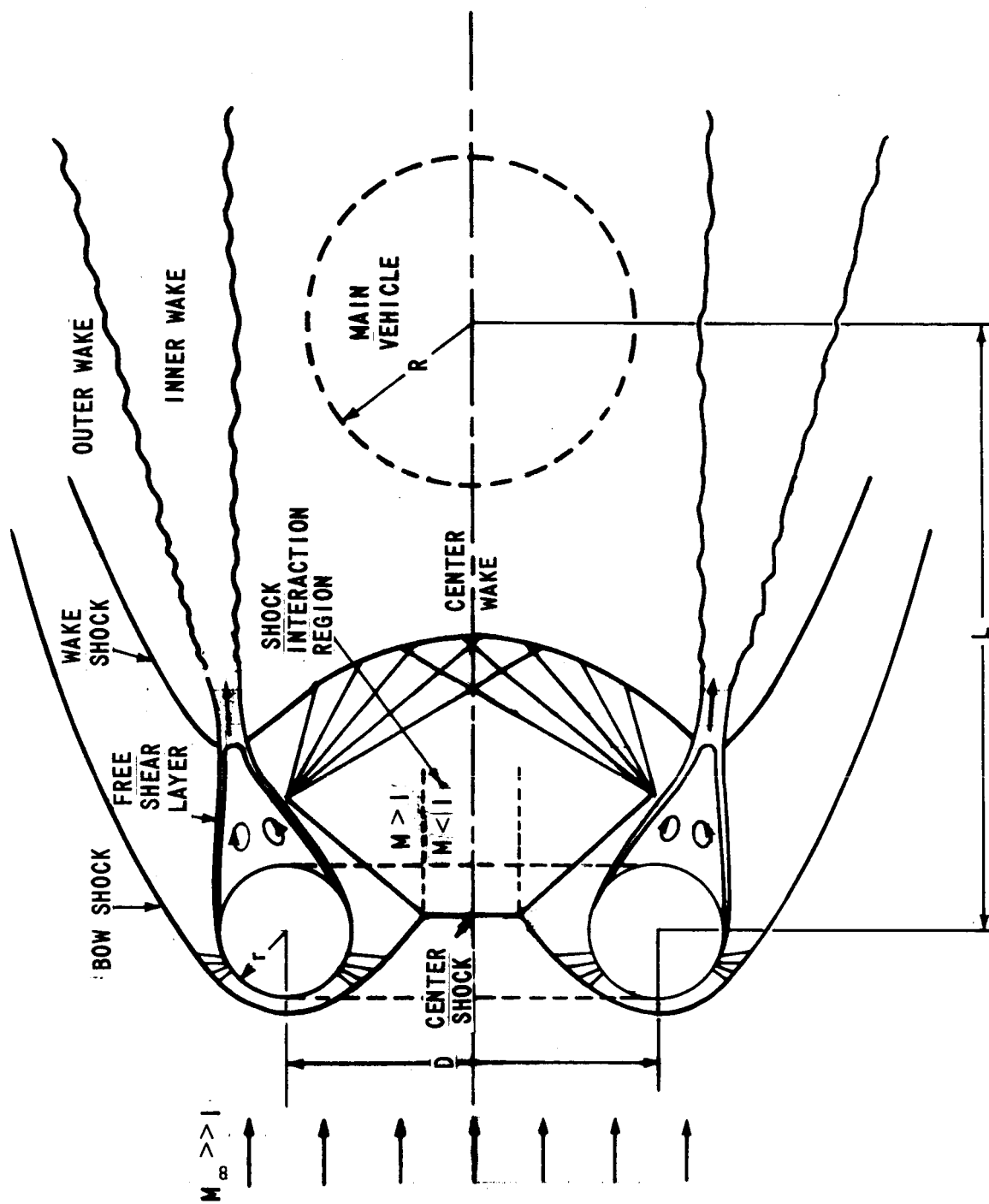


FIGURE 4 - FLOW AROUND A HYPERSONIC TORUS

BELLCOMM, INC.

Subject: A New Concept in Heat Shield
Design - Deployable Heat
Shield - Case 710

From: C. P. Wang

Distribution List

NASA Headquarters

Messrs. W. O. Armstrong/MTX
F. P. Dixon/MTY
E. W. Hall/MTG
D. P. Hearth/SL
T. A. Keegan/MA
R. S. Kraemer/SL
D. R. Lord/MTD
D. G. Rea/SL
A. D. Schnyer/MTV
J. W. Wild/MTE

Ames Research Center

Mr. L. Roberts/M (2)

Langley Research Center

Messrs. J. S. Martin
I. Taback

Bellcomm, Inc.

Messrs. F. G. Allen
G. M. Anderson
A. P. Boysen, Jr.
D. A. Chisholm
J. P. Downs
D. R. Hagner
P. L. Havenstein
N. W. Hinnners
B. T. Howard
D. B. James
J. Kranton
K. E. Martersteck
R. K. McFarland
J. Z. Menard
G. T. Orrok
T. L. Powers
I. M. Ross
F. N. Schmidt

Bellcomm, Inc. (Cont'd)

R. L. Selden
R. V. Sperry
W. B. Thompson
J. W. Timko
J. M. Tschirgi
R. L. Wagner
J. E. Waldo

All members, Division 101
Department 1023
Central Files
Library